Identification and functional analyses of disease-associated P4-ATPase phospholipid flippase variants in red blood cells

Received for publication, December 20, 2018, and in revised form, March 6, 2019 Published, Papers in Press, March 8, 2019, DOI 10.1074/jbc.RA118.007270

Angela Y. Liou[‡], Laurie L. Molday[‡], Jiao Wang[‡1], Jens Peter Andersen[§], and Robert S. Molday[‡2]

From the [‡]Department of Biochemistry and Molecular Biology, University of British Columbia, Vancouver, British Columbia V6T 1Z3, Canada and [§]Department of Biomedicine, Aarhus University, Ole Worms Allé 4, Building 1160, DK-8000 Aarhus C, Denmark

Edited by George M. Carman

ATP-dependent phospholipid flippase activity crucial for generating lipid asymmetry was first detected in red blood cell (RBC) membranes, but the P4-ATPases responsible have not been directly determined. Using affinity-based MS, we show that ATP11C is the only abundant P4-ATPase phospholipid flippase in human RBCs, whereas ATP11C and ATP8A1 are the major P4-ATPases in mouse RBCs. We also found that ATP11A and ATP11B are present at low levels. Mutations in the gene encoding ATP11C are responsible for blood and liver disorders, but the disease mechanisms are not known. Using heterologous expression, we show that the T415N substitution in the phosphorylation motif of ATP11C, responsible for congenital hemolytic anemia, reduces ATP11C expression, increases retention in the endoplasmic reticulum, and decreases ATPase activity by 61% relative to WT ATP11C. The I355K substitution in the transmembrane domain associated with cholestasis and anemia in mice was expressed at WT levels and trafficked to the plasma membrane but was devoid of activity. We conclude that the T415N variant causes significant protein misfolding, resulting in low protein expression, cellular mislocalization, and reduced functional activity. In contrast, the I355K variant folds and traffics normally but lacks key contacts required for activity. We propose that the loss in ATP11C phospholipid flippase activity coupled with phospholipid scramblase activity results in the exposure of phosphatidylserine on the surface of RBCs, decreasing RBC survival and resulting in anemia.

The asymmetrical distribution of lipids across membranes of eukaryotic cells plays a crucial role in many cellular processes, including blood coagulation, apoptosis, phagocytosis, vesicle trafficking, axon elongation, sensory functions, and metabolic homeostasis among others (1–4). Two classes of ATP-dependent lipid transporters have been implicated in the generation and maintenance of phospholipid asymmetry in eukaryotic cells (5, 6): P4-ATPases, a subfamily of P-type ATPases, transport phospholipids from the exoplasmic (extracellular or lumen) to the cytoplasmic leaflet of cell membranes (7), and some ATP-binding cassette (ABC) transporters transport specific phospholipids most often in the opposite direction (8). A third class of ATP-independent phospholipid transporters, scramblases, when active, serve to dissipate phospholipid asymmetry, a process important in such cellular processes as blood coagulation, apoptosis, and phagocytosis (9, 10). The importance of phospholipid transporters in generating, maintaining, and dissipating lipid asymmetry is evident in the finding that loss-in-function mutations in these transporters have been linked to severe human and rodent disorders, including anemia, blood clotting dysfunction, cholestasis, neurodegenerative diseases, sensory disorders, and ataxia among others (11–20).

Transbilayer lipid asymmetry was first characterized in red blood cells (RBCs)[3] using a variety of chemical and biochemical techniques (21–24). Phosphatidylserine (PS) and phosphatidylethanolamine (PE) were found to be preferentially, if not exclusively, localized on the inner or cytoplasmic leaflet of the RBC plasma membrane, whereas phosphatidylcholine (PC), sphingomyelin, and glycolipids were primarily confined to the external or exocytoplasmic leaflet. Because the hydrophobic lipid bilayer serves as a high energy barrier for movement of the polar headgroups of phospholipids across membranes, it was proposed that membrane proteins generally known as flippases or translocases must provide a low energy pathway for the transport or flipping of membrane phospholipids across the bilayer. Early studies showed that human RBCs contain a membrane protein initially referred to as an aminophospholipid translocase that actively transported PS and PE across the plasma membrane (23, 25–28). An aminophospholipid translocase that also uses PS and PE as substrates was subsequently identified and cloned from bovine chromaffin granules (29, 30).

This work was supported by Canadian Institutes of Health Research Grant PJT 148649 (to R. S. M.), National Institutes of Health Grant EY002422 (to R. S. M.), and Danish Council for Independent Research Grant DFF-6110-00271 (to J. P. A.). The authors declare that they have no conflicts of interest with the contents of this article. The content is solely the responsibility of the authors and does not necessarily represent the official views of the National Institutes of Health.

The mass spectrometry proteomics data have been deposited to the ProteomeXchange Consortium via the PRIDE partner repository with the dataset identifier PXD011841.

[1] Present address: Laboratory of Molecular Neural Biology, School of Life Sciences, Shanghai University, 200444 Shanghai, China.

[2] To whom correspondence should be addressed: Dept. of Biochemistry and Molecular Biology, 2350 Health Sciences Mall, University of British Columbia, Vancouver, British Columbia V6T 1Z3, Canada. Tel.: 604-822-6173; Fax: 604-822-5227; E-mail: molday@mail.ubc.ca.

[3] The abbreviations used are: RBC, red blood cell; PS, phosphatidylserine; PE, phosphatidylethanolamine; PC, phosphatidylcholine; MS/MS, tandem mass spectrometry; ER, endoplasmic reticulum; WGA, wheat germ agglutinin; HEK293T, human embryonal kidney 293T; CAMRQ, cerebellar ataxia, mental retardation, and dysequilibrium syndrome; DOPC, 1,2-dioleoyl-*sn*-glycero-3-phosphocholine; DOPS, 1,2-dioleoyl-*sn*-glycero-3-phosphoserine; TM, transmembrane; SERCA, sarcoplasmic reticulum Ca^{2+}-ATPase; DAPI, 4′,6-diamidino-2-phenylindole.

© 2019 Liou et al. Published under exclusive license by The American Society for Biochemistry and Molecular Biology, Inc.

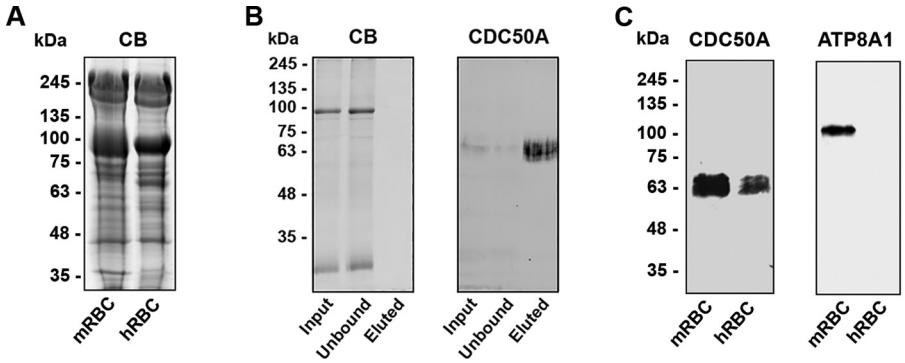

Figure 1. SDS–gel electrophoresis and Western blots of P4-ATPase–CDC50A complex from RBC membranes. *A*, SDS gels of human (*hRBC*) and mouse (*mRBC*) RBC membranes stained with Coomassie Blue (*CB*). Approximately 30 μg of protein was applied to each lane. *B*, SDS–gel electrophoresis of fractions derived from immunoaffinity purification of CDC50A from RBC membranes. RBC membranes were solubilized in CHAPS/Mega-10 detergent and depleted of spectrin and other cytoskeletal proteins. The detergent-solubilized extract was applied to a Cdc50–7F4 immunoaffinity column, and after removal of the unbound protein, the bound P4-ATPase–CDC50A complex was eluted with the Cdc50 peptide. The input, unbound, and bound fractions were analyzed on SDS gels stained with Coomassie Blue (*CB*) and Western blots labeled with the Cdc50–7F4 antibody. *C*, Western blots of immunoaffinity-purified P4-ATPase complexes labeled for CDC50A with the Cdc50–7F4 mAb and ATP8A1 with a polyclonal antibody.

This protein, originally called ATPase II, is now known as ATP8A1, a member of the P4-ATPase subfamily of P-type ATPases.

Because the aminophospholipid translocase detected in RBC membranes had a similar substrate specificity as ATP8A1 of chromaffin granules, it was generally thought that ATP8A1 was the principal aminophospholipid flippase in human and mouse RBCs (31). This was supported by the finding that ATP8A1 was detected in mouse RBC membranes by Western blotting (32). However, the RBCs of mice deficient in ATP8A1 appeared normal and did not expose PS on their cell surface (33). More recently, RBCs of mice with mutations in the gene encoding the P4-ATPase ATP11C were reported to have an abnormal shape, reduced life span, and increased exposure of surface PS that further increased with age, resulting in anemia (12). Recent genetic studies have also pointed to ATP11C as an important P4-ATPase in human RBCs (34). In this study, an individual with a missense mutation in ATP11C was observed to display a mild form of congenital hemolytic anemia. RBCs of this individual did not have abnormal shapes or significant increases in PS exposure on their surface, but they did display a 10-fold decrease in internalization of added PS relative to RBCs from normal individuals.

Although these studies provide support for a role of ATP11C in erythrogenesis, direct identification and relative abundance of various P4-ATPase(s) in membranes of mature mammalian RBCs have been elusive due in part to the low copy number of P4-ATPases and the fact that mammalian RBCs do not contain a nucleus for genetic analysis. The human genome contains 14 genes that encode P4-ATPases (the mouse genome contains 15 P4-ATPases). Twelve P4-ATPases are known to interact with CDC50 (also known as TMEM30), an accessory or β-subunit that plays a crucial role in the expression, subcellular localization, and functional activity of phospholipid flippases (1, 13, 35–38). There are three CDC50 variants, CDC50A, CDC50B, and CDC50C (39). Recent proteomic studies have shown that most tissues, including brain, retina, testis, kidney, and liver, contain multiple P4-ATPases that associate with the CDC50A variant (38).

In this study, we have purified P4-ATPase–CDC50A complexes from human and mouse RBC membranes by immunoaffinity chromatography and identified these complexes by mass spectrometry (MS). We show that ATP11C and ATP8A1 are the predominant P4-ATPases in mouse RBCs, whereas ATP11C is the only abundant P4-ATPase in human RBCs. We also examined the expression and functional activity of ATP11C mutants associated with human and rodent blood disorders to obtain insight into the molecular basis for these diseases.

Results

Detection of CDC50A and ATP8A1 in RBC membranes

Membranes isolated from hypotonically lysed human and mouse RBCs were used as the starting material for the analysis of P4-ATPase–CDC50A complexes. Fig. 1*A* shows a typical Coomassie Blue–stained gel of RBC membrane proteins resolved by SDS-PAGE. The Cdc50–7F4 mAb, which binds to a conserved epitope (AKDEVDGGP) near the N terminus of CDC50A (37), was used to isolate P4-ATPase–CDC50A complexes from RBC membranes. Detergent-solubilized RBC membranes depleted of the spectrin-containing cytoskeletal system were applied to an immunoaffinity matrix consisting of the Cdc50–7F4 antibody coupled to Sepharose (38). After removal of unbound protein, the bound protein was eluted from the matrix with the competing 7F4 peptide for analysis by SDS–gel electrophoresis and Western blotting. Fig. 1*B* shows a Coomassie Blue–stained gel and a Western blot of the input, unbound, and eluted CDC50A fraction from detergent-solubilized mouse RBC membranes.

As shown in Fig. 1*C*, CDC50A isolated from mouse and human RBC membranes migrated as relatively broad bands with an apparent molecular mass of 60–70 kDa as reported previously in other tissues (38). The diffuse nature of the band is most likely due to variable glycosylation of CDC50A. The presence of ATP8A1 in the eluted fraction from the CDC50A immunoaffinity matrix was also investigated by Western blotting (Fig. 1*C*). ATP8A1 was detected as a protein having an

Table 1

Mass spectrometric analysis of P4-ATPases in mouse and human RBCs

Identity and quantification based on spectral intensity of P4-ATPase–CDC50A complexes were determined from MS/MS measurements in two independent experiments. Detergent-solubilized human and mouse RBC membranes (~3 mg) were applied to a Cdc50-7F4 immunoaffinity column. After removing the unbound protein, the P4-ATPase–CDC50A complexes were eluted with the 7F4 competing peptide. The eluted fraction was subjected to trypsin digestion using the filter-aided sample preparation procedure, and the tryptic peptides were analyzed by tandem MS/MS. Intensity (%) was obtained by taking the fraction of the spectral intensity of the selected P4-ATPase to the total spectral intensity of all P4-ATPases detected in the tissue.

RBCs	Protein ID	Protein name	Sequence length	Peptides Exp. 1/Exp. 2	Sequence coverage Exp. 1/Exp. 2	Intensity of total P4-ATPase Exp. 1/Exp. 2
					%	%
Human	Q9NV96	CDC50A/TMEM30A	361	5/8	17.4/29.6	
	Q8NB49	ATP11C	1132	16/22	14.2/26.4	90/84
	Q9Y2G3	ATP11B	1177	2/12	2.2/10.4	8/11
	P98196	ATP11A	1134	3/6	2.9/5.6	2/5
Mouse	Q8VEK0	CDC50A/TMEM30A	364	18/19	41.2/39.3	
	P70704	ATP8A1	1116	58/38	51.2/38	63/60
	Q9QZW0	ATP11C	1129	50/38	41.1/35.8	36/39
	Q6DFW5	ATP11B	1175	16/18	15.2/15.6	1/1
	Q8K2X1	ATP10D	1416	12/2	9.2/2.3	0.3/0.07

apparent molecular mass of 125 kDa in mouse RBC membranes but was undetectable in human RBC membranes.

Identification and quantification of P4-ATPase–CDC50A complexes in RBC membranes by MS

To identify both high- and low-abundance P4-ATPase–CDC50A complexes from RBC membranes, the peptide-eluted fraction from the CDC50A immunoaffinity matrix was digested with trypsin, and the peptides were analyzed by LC-tandem MS (MS/MS). Table 1 summarizes the P4-ATPase–CDC50A complexes identified from human and mouse RBC membranes and their relative abundance in two independent experiments. CDC50A was present in both human and mouse RBC membranes with average sequence coverages of 24 and 40% for the human and mouse proteins, respectively. The predominant P4-ATPase in human RBC membranes was ATP11C, making up over 87% of the P4-ATPase–CDC50A complexes based on spectral intensities. In mouse RBC membranes, the principal P4-ATPases were ATP8A1 and ATP11C, comprising over 62 and 37% of the total P4-ATPase–CDC50A complexes, respectively. ATP11B (~9%) and ATP11A (~4%) were present in lower abundance in human RBC membranes, and ATP11B (~1%) was detected in mouse RBC membrane preparations. Trace amounts of ATP10D were also detected in both mouse RBC membrane preparations and may represent contaminants from other cells. P4-ATPase–CDC50A complexes were not detected in a control study in which detergent-solubilized mouse RBC membranes were applied to an immunoaffinity matrix in which the Cdc50–7F4 antibody was replaced with an irrelevant mAb (dataset available in PRIDE repository; see "Experimental procedures").

In addition to P4-ATPase–CDC50A complexes, other RBC proteins were also present in the dataset (dataset available in the PRIDE repository; see "Experimental procedures"). These proteins may represent interacting proteins or minor contaminants in the purified protein preparations. Further studies are needed to delineate between these possibilities.

Expression and localization of the T415N missense mutation in ATP11C associated with congenital hemolytic anemia

A recent study has identified a T418N mutation of human ATP11C that causes a relatively mild form of congenital hemolytic anemia (34). The effect of this mutation on the expression and functional activity of ATP11C, however, had not been determined. Threonine 418 is located in a highly conserved motif within the phosphorylation or P domain of P-type ATPases (Fig. 2, *A* and *B*). To determine the effect of this mutation on ATP11C, we generated a mouse ATP11C construct containing a C-terminal 1D4 epitope used for detection and purification and the T415N mutation corresponding to the human T418N mutation. The T415S and T415A mutants were also produced to study the effects of these substitutions on the properties of ATP11C. Wildtype (WT) ATP11C and mutants were coexpressed with CDC50A in HEK293T cells, and the level of expression of the CHAPS-solubilized proteins after removal of insolubilized protein was determined by Western blotting. As shown in Fig. 2*C*, the level of expression of T415S was comparable with WT ATP11C. In contrast, the T415N mutant was expressed at ~59% and T415A was expressed at 32% of WT ATP11C. The expressed ATP11C variants were then purified on a Rho-1D4 immunoaffinity column. Fig. 2*D* shows a Coomassie Blue–stained SDS gel and a Western blot of the purified protein complexes. CDC50A subunit copurified with the ATP11C variants, indicating that the immunoaffinity-isolated Thr-415 mutants assembled with CDC50A. The expression levels of the mutants after purification was similar to that before purification (Fig. 2, *C* and *E*).

Most P4-ATPases require the association with its β-subunit, CDC50, for proper folding, exit from the endoplasmic reticulum (ER), and formation of a functional flippase complex (37, 40–42). In the absence of CDC50, P4-ATPases are retained in the ER as misfolded proteins by the quality control system of cells (37, 43). In this study, we first analyzed the cellular localization of WT ATP11C in COS-7 cells with and without cotransfection with CDC50A by immunofluorescence imaging. ATP11C showed significant colocalization with the plasma membrane marker wheat germ agglutinin (WGA) in cells cotransfected with CDC50A. ATP11C that was present inside the cell showed limited colocalization with the ER marker calnexin. In contrast, in the absence of CDC50A transfection, ATP11C was largely retained in the cell and predominantly colocalized with the ER marker calnexin (Fig. 3*A*).

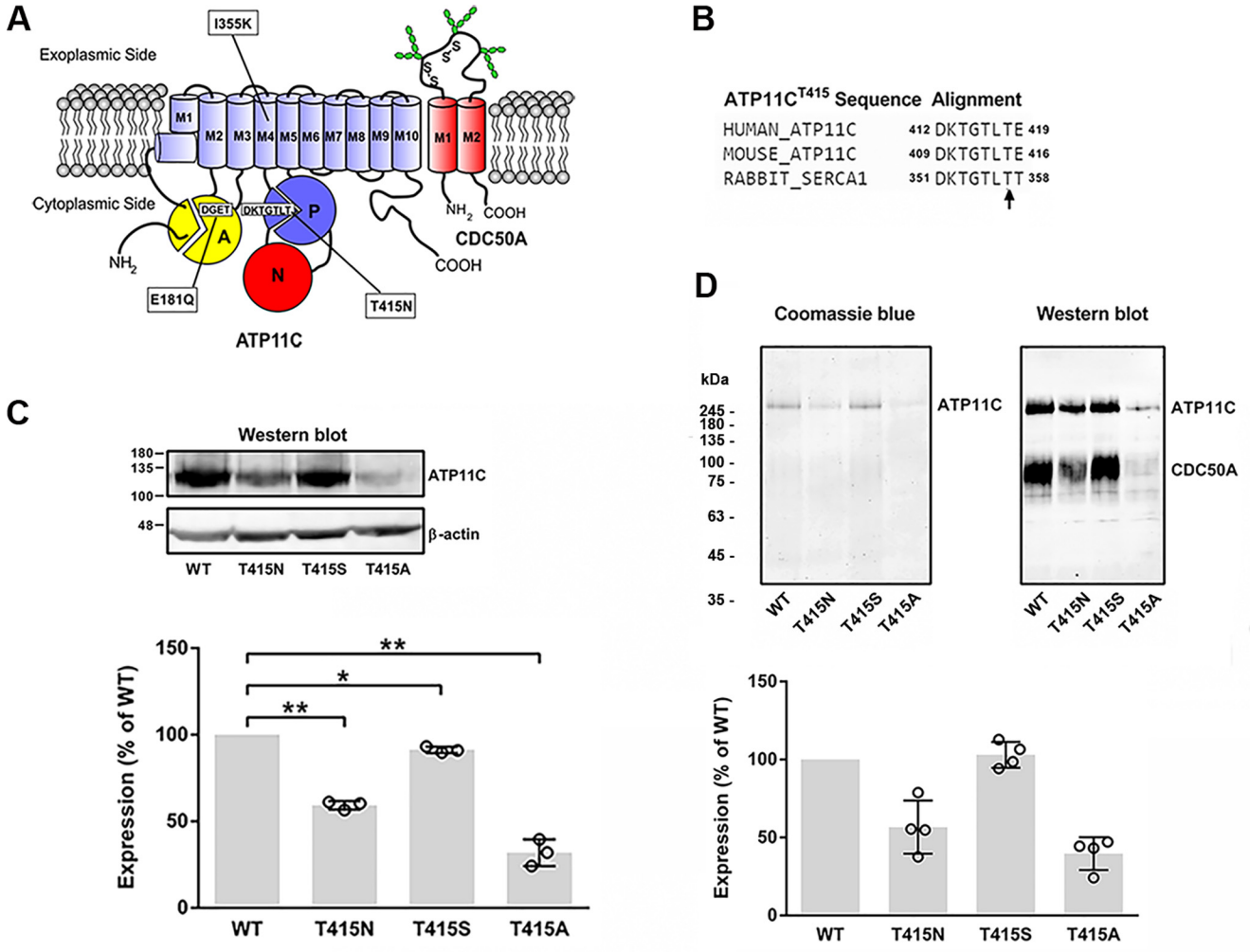

Figure 2. Expression and purification of WT ATP11C and Thr-415 mutants coexpressed with CDC50A. *A*, topological model for ATP11C–CDC50A complex showing the predicted transmembrane segments, phosphorylation or P domain containing the phosphorylation motif (DKTGTLT), actuator or A domain containing the dephosphorylation motif (DGET), and nucleotide-binding or N domain together with the location of selected mutations in ATP11C examined in this study. *B*, sequence alignment of the highly conserved phosphorylation site containing the disease-associating threonine in human ATP11C (*arrow* denotes Thr-418 residue in human, Thr-415 residue in mouse, and Thr-357 residue in SERCA1). *C*, expression levels of the ATP11C variants relative to WT ATP11C after solubilization of the cells with CHAPS detergent. *Upper panel*, example of a Western blot of the ATP11C variants. β-Actin was used as a loading control. *Lower panel*, quantification of expression levels observed from the Western blots. Data are the average values with *error bars* representing ± S.D. for $n = 3$. *, $p = 0.0137$ for WT *versus* T415S; **, $p = 0.0012$ for WT *versus* T415N; **, $p = 0.0042$ for WT *versus* T415A. *D*, *upper panel*, Coomassie Blue–stained gel and Western blots of ATP11C coexpressed with CDC50A in HEK293T cells and purified on a Rho-1D4 immunoaffinity column. The ATP11C protein was readily detected by Coomassie Blue staining as a band at approximate molecular mass of 125 kDa; the CDC50A appeared as a faint diffuse band in the molecular mass range of 60–70 kDa. Western blots labeled for ATP11C with the Rho-1D4 antibody and CDC50A with the Cdc50–7F4 antibody confirmed the identity of the proteins. *Lower panel*, quantification of Thr-415 mutants relative to WT ATP11C. WT ATP11C and mutants were isolated on an immunoaffinity matrix and quantified from Western blots. T415N was expressed at about 57% and T415A mutant was expressed at about 37% of WT levels, whereas T415S mutant was expressed at a level comparable with WT ATP11C. Data are the average values with *error bars* representing ± S.D. for $n = 3$.

The lower levels of expression observed for T415N and T415A raised the possibility that a significant fraction of these mutants is highly misfolded and retained in the ER even when coexpressed with CDC50A. This was confirmed by immunofluorescence staining. T415N and T415A mutants showed more limited colocalization with WGA. Instead, a significant fraction of these mutants was localized to the perinuclear region of the cell where they colocalized with calnexin (Fig. 3*A*). In contrast, T415S immunostaining displayed significant overlap with WGA staining in the plasma membrane of transfected cells and limited colocalization with the calnexin. These results indicate that the T415S mutant was able to exit the ER and traffic to the plasma membrane similarly to WT ATP11C, whereas T415N and T415A showed reduced exit from the ER and trafficking to the plasma membrane.

To further examine the effect of these missense mutations on the extent to which these Thr-415 variants trafficked to the plasma membrane, we biotin-labeled the surface of cells cotransfected with the Thr-415 variants and CDC50A. Fig. 3*B* shows that the T415N and T415A variants showed reduced cell surface labeling relative to WT ATP8A2. The T415S mutant showed a statistically similar level of surface labeling as the WT protein.

ATPase activity of the Thr-415 variants

The ATPase activities of the purified complexes in the presence of 100% 1,2-dioleoyl-*sn*-glycero-3-phosphocholine

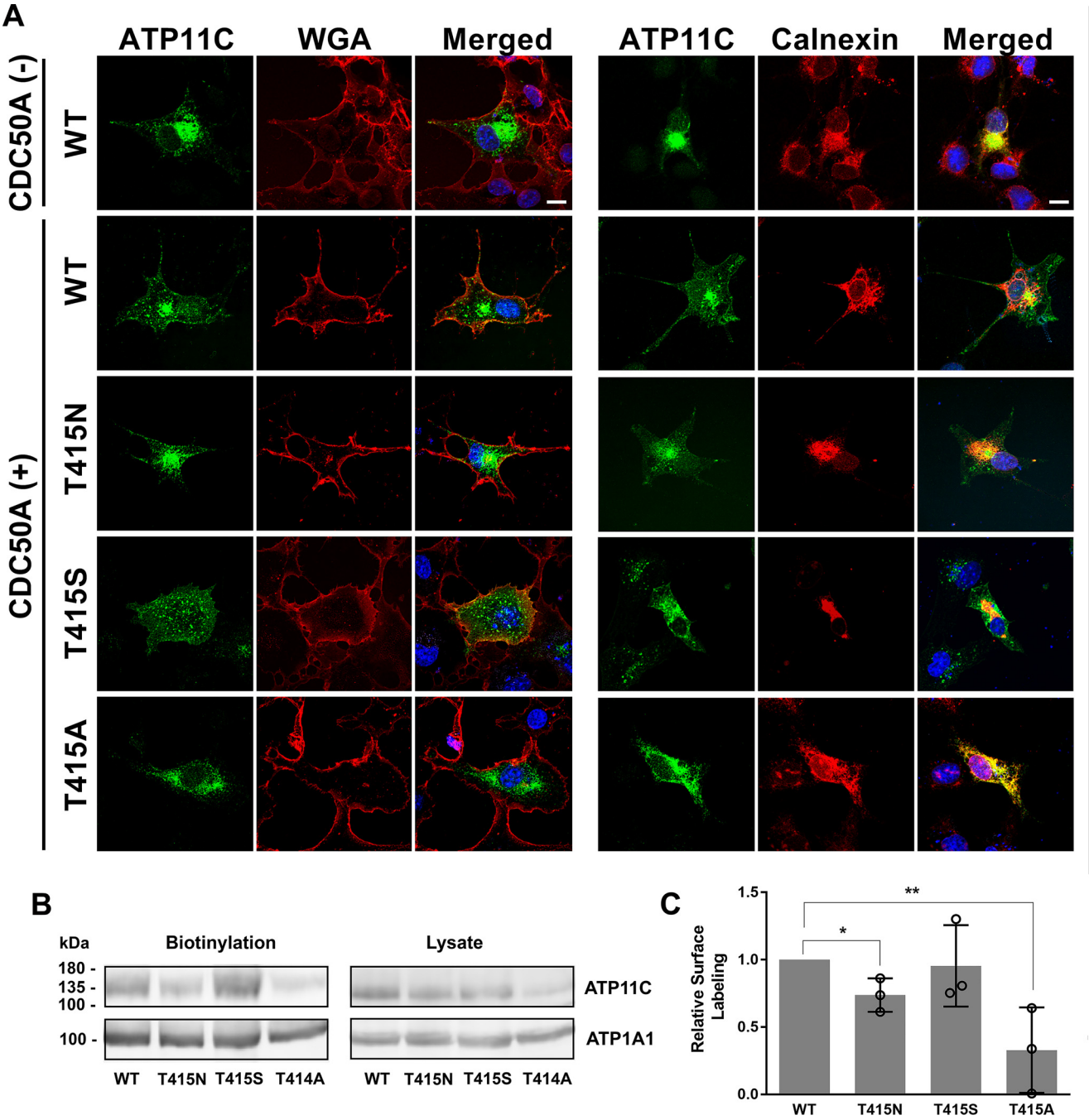

Figure 3. Immunofluorescence localization and surface labeling of ATP11C Thr-415 mutants. *A*, WT ATP11C and mutants were expressed in COS-7 cells in the presence (+) or absence (−) of CDC50A. *Left panel*, cells were labeled for ATP11C (*green*) and WGA (*red*) and counterstained with the nuclear stain DAPI (*blue*) for fluorescence microscopy. *Right panel*, cells were labeled for ATP11C (*green*) and the ER marker calnexin (*red*) and counterstained with DAPI (*blue*). T415N and T415A showed a higher degree of colocalization with calnexin than WT or T415S for cells cotransfected with CDC50A. *Scale bars*, 10 μm. *B*, example of Western blots of HEK293T cells coexpressing ATP11C variants and CDC50A and surface-labeled with biotin (*Biotinylation*). The blots were labeled for ATP11C and Na/K-ATPase ATP1A1 as a control. Cell lysate is also shown. *C*, quantitative analysis of biotin surface labeling of the ATP11C mutants relative to WT ATP11C. Data are average values with *error bars* representing ± SD for $n = 3$. *, $p = 0.0217$ for WT *versus* T415N; **, $p = 0.0214$ for WT *versus* T415A. The difference between WT ATP11C and the T415S mutant was not significant.

(DOPC) and 20% 1,2-dioleoyl-*sn*-glycero-3-phosphoserine (DOPS) and 80% DOPC were measured to assess the functional properties of the Thr-415 mutants. As shown previously (38), the ATPase activity of WT ATP11C, which correlates with ATP-dependent PS flippase activity, was strongly activated by DOPS (Fig. 4*A*). The DOPS-activated ATPase activity of the T415N mutant was reduced to 39% of WT ATP11C, and the activity of the T415A mutant was reduced by more than 4-fold relative to WT ATP11C. In contrast, the DOPS-activated ATPase activity was higher for the T415S mutant than WT ATP11C. The effect of increasing DOPS concentration on the activity of WT ATP11C and its T415N and T415A mutants is shown in Fig. 4*B*. All proteins showed typical substrate saturation curves with the following parameters: WT, K_a of 19 ± 3 μM (PS) and V_{max} of 19.9 ± 0.6 μmol of ATP hydrolyzed/min/mg of protein ($n = 4$); T415N mutant,

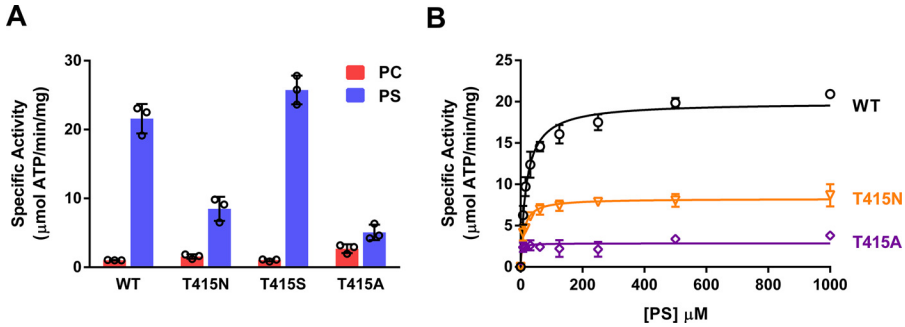

Figure 4. ATPase activity of WT ATP11C and Thr-415 mutants. WT ATP11C and the mutants were coexpressed with CDC50A and purified on a Rho-1D4 immunoaffinity matrix. *A*, specific ATPase activity was measured in 100% DOPC (*PC*) and 80% DOPC and 20% DOPS (*PS*). Data are the average values with *error bars* representing ± S.D. for $n = 3$. *B*, effect of DOPS (*PS*) concentration on the ATPase activity of WT and T415N and T415A mutants. Curves were fitted with Michaelis–Menten kinetics. Measurements were done in triplicates. Data for WT ATP11C were for $n = 4$; *Error bars* represent S.D. mutants were for $n = 2$ independent experiments.

K_a of 10 ± 2 μM (PS) and V_{max} of 8.3 ± 0.3 μmol of ATP hydrolyzed/min/mg of protein ($n = 2$); and T415A mutant, K_a of 2 ± 2 μM (PS) and V_{max} of 2.9 ± 0.3 μmol of ATP hydrolyzed/min/mg of protein ($n = 2$).

Collectively, our studies indicate that the T415N and T415A mutations result in reduced expression as measured by solubilization with CHAPS, decreased localization in the plasma membrane, and increased retention within the ER. Coimmunoprecipitation studies indicate that CDC50A interacts with the fraction of the mutants that is solubilized by CHAPS detergent, but the PS-activated ATPase activity is significantly lower than that of WT ATP11C.

Expression, localization, and ATPase activity of the ATP11C I355K mutation associated with blood disorders and cholestasis in mice

Mutations in ATP11C have been reported to cause defective B-cell development, anemia, and cholestasis in several mouse lines (12, 15, 16, 44). One strain of mice was shown to have an I355K mutation within the transmembrane domain (Fig. 2*A*). To determine the effect of this missense mutation on ATP11C, we coexpressed WT ATP11C and the I355K mutant with CDC50A in HEK293T cells. The I355A and I355V mutants were also analyzed to further define the effect of these amino acid substitutions on the properties of ATP11C. The E181Q ATPase-deficient mutant was included as a negative control for ATPase activity (38). As shown on Coomassie Blue–stained SDS gels and Western blots, all the ATP11C mutants were expressed at levels similar to WT ATP11C and copurified with CDC50A (Fig. 5, *A* and *B*).

The effect of these mutations on the distribution of ATP11C–CDC50A complexes was investigated by immunofluorescence microscopy. All mutants displayed a strong overlap with WGA staining, similar to the cellular distribution of WT ATP11C (Fig. 5*C*).

Next, we measured the ATPase activities of the purified ATP11C–CDC50A complexes in the presence of 100% DOPC and 20% DOPS, 80% DOPC. The I355K disease-associated mutant, like the E181Q ATPase-deficient mutant, showed essentially baseline activity in the presence or absence of DOPS (Fig. 5*D*). The DOPS-stimulated ATPase activity was largely retained when isoleucine was replaced with valine at position 355 but was reduced by up to 66% when isoleucine was substituted with alanine. To further evaluate the activity of these mutants, we examined the effect of increasing DOPS concentrations on their DOPS-stimulated ATPase activity. Fig. 5*E* shows that, like WT ATP11C, the I355A mutant displayed typical PS saturation curves with half-maximum activation constants of K_a (PS) of 16 ± 3 μM for I355A mutant and a V_{max} of 7.1 ± 0.3 μmol of ATP hydrolyzed/min/mg of protein ($n = 3$). Although the I355K mutant showed very low activity, it was possible to obtain the following kinetic parameters: K_a (PS) of 80 ± 39 μM and V_{max} of 0.6 ± 0.1 μmol of ATP hydrolyzed/min/mg of protein ($n = 2$). In bovine ATP8A2, the mutation I362A corresponding to I355A in ATP11C showed similar trend in kinetic parameters relative to the WT protein with a 60% reduction in the V_{max} and a 1.6% reduction in K_a for PS (45).

Analysis of the ATP11C V357M mutation

The I355K mutation is located in transmembrane 4 (TM4) of murine ATP11C (Fig. 2*A*), a segment that has been implicated in the transport of substrates in P-type ATPases (45–48). Another mutation, I376M, in TM4 of ATP8A2 has been reported to cause cerebellar ataxia, mental retardation, and dysequilibrium syndrome (CAMRQ) in a Turkish family (17). This mutation (I364M in bovine ATP8A2) shows a significant loss in both PS-activated ATPase activity and ATP-dependent transport activity of PS (45, 49). Because ATP11C and ATP8A2 both transport PS and PE, it was of interest to determine whether a mutation in the corresponding residue of ATP11C (V357M) has a similar effect on the activity of ATP11C. Analysis of the ATP11C mutants coexpressed with CDC50A in HEK293T cells showed that the V357M and V357I mutations had no significant effect of the expression level or localization of ATP11C (Fig. 6, *A* and *B*). Furthermore, functional studies indicated that these mutants retained significant PS-stimulated ATPase activity (Fig. 6*C*). The V357M mutant showed a 24% reduction in specific activity and V357I displayed a 24% increase in activity relative to WT ATP11C.

Discussion

This is the first study designed to directly identify high- and low-abundance P4-ATPases–CDC50A complexes in human and mouse RBCs. Using an immunoaffinity approach in conjunction with MS, we have shown that ATP11C is the only major

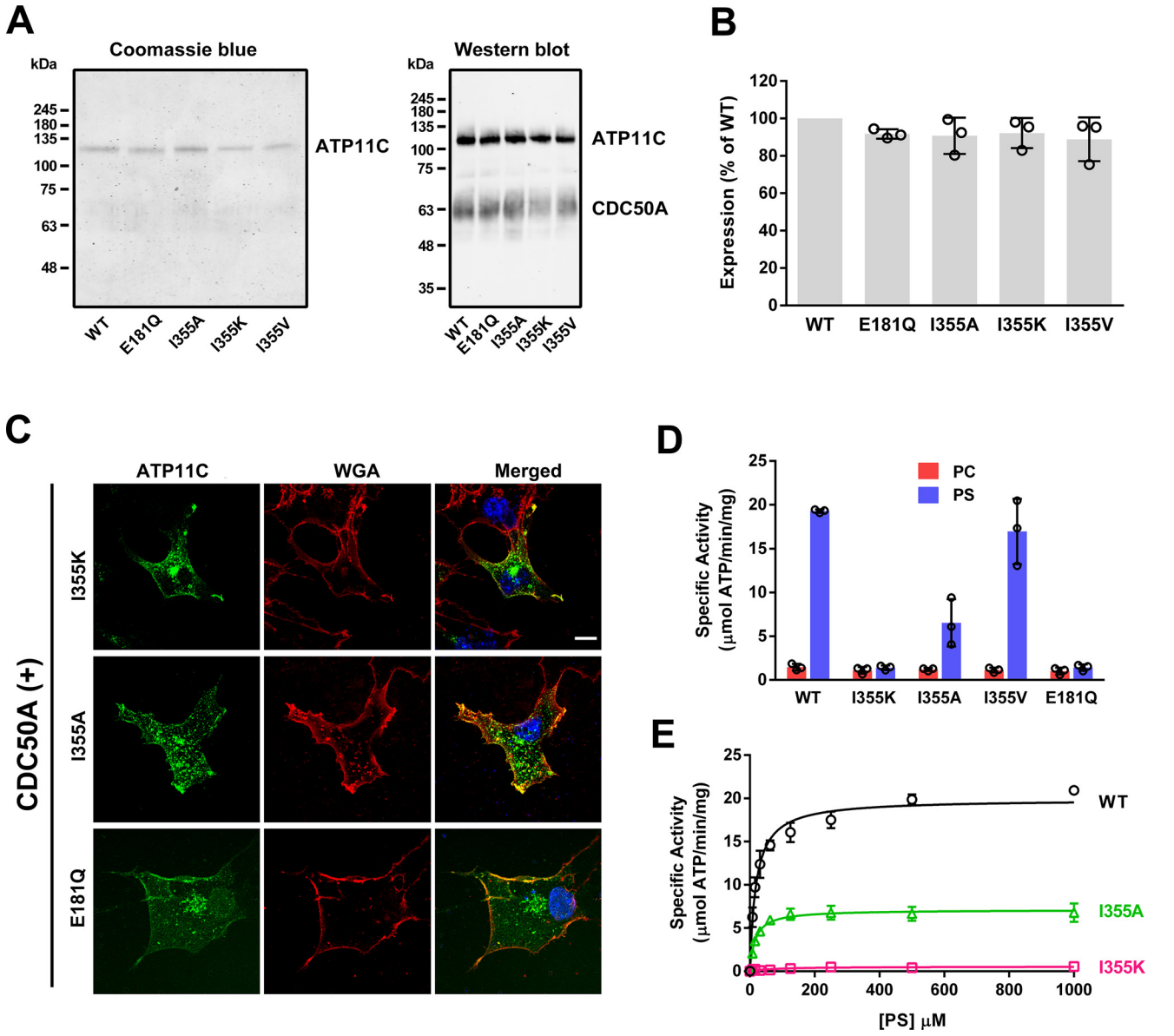

Figure 5. Expression, localization, and ATPase activity of ATP11C Ile-355 mutants. *A*, immunoaffinity-purified ATP11C–CDC50A complexes were separated on SDS-polyacrylamide gels and stained with Coomassie Blue. Western blots were labeled for ATP11C with the Rho-1D4 antibody and CDC50A with the Cdc507F4 antibody. *B*, the expression of WT ATP11C and mutants was quantified from Western blots. All constructs were expressed and purified at similar levels as WT ATP11C. Data are the average values with *error bars* representing ± S.D. for $n = 3$. *C*, COS-7 cells coexpressing ATP11C mutants and CDC50A were labeled for ATP11C with the Rho-1D4 antibody (*green*) and WGA (*red*) and counterstained with DAPI (*blue*). The ATPase-deficient E181Q mutant, disease-causing I355K mutant, and I355A mutant localized to the plasma membrane like WT ATP11C. *Scale bar*, 10 μm. *D*, the ATPase activity of the immunoaffinity-purified ATP11C mutants was measured in 100% DOPC (*PC*) and in 80% DOPC and 20% DOPS (*PS*). WT ATP11C and the I355V mutant had similar PS-activated ATPase activity; I355K, like the ATPase-deficient E181Q, was largely devoid of activity; and the I355A mutant had about 34% of WT activity. Data are an average values with *error bars* representing ± S.D. *E*, the effect of increasing DOPS concentration on the activity of WT ATP11C ($n = 4$) and the I355A ($n = 3$) and I355K ($n = 2$) mutants. Curves were fitted with Michaelis–Menten kinetics. Data are average values with *error bars* representing S.D.

P4-ATPase flippase in human RBCs, whereas both ATP8A1 and ATP11C are relatively abundant flippases in mouse RBCs. In addition to these P4-ATPases, ATP11A and ATP11B are also present in human RBCs, and ATP11B was detected at low levels in mouse RBCs (Table 1). Western blotting confirmed our proteomic studies, showing the presence of ATP8A1 in mouse RBC membranes in agreement with a previous study (32) and the absence of detectable ATP8A1 in human RBCs.

P4-ATPases were not detected in previously reported "deep coverage" mass spectrometry–based proteomic studies of human and mouse RBCs, presumably due to the low quantity of these flippases in RBCs (50, 51). However, inspection of a more recent proteomic dataset of human RBCs utilizing improved sample preparation techniques and highly sensitive instrumentation revealed the presence of three P4-ATPases (ATP11C, ATP11A, and ATP11B) with ATP11C comprising over 80% of the P4-ATPases (52), consistent with our analysis presented in Table 1. This proteomic dataset also revealed a low copy number for these flippases with the most abundant P4-ATPase ATP11C having an average copy number of only 2230 ± 1147 ($n = 4$) per human RBC (52). Other P4-ATPases, including ATP9A and ATP9B, which do not associate with CDC50 pro-

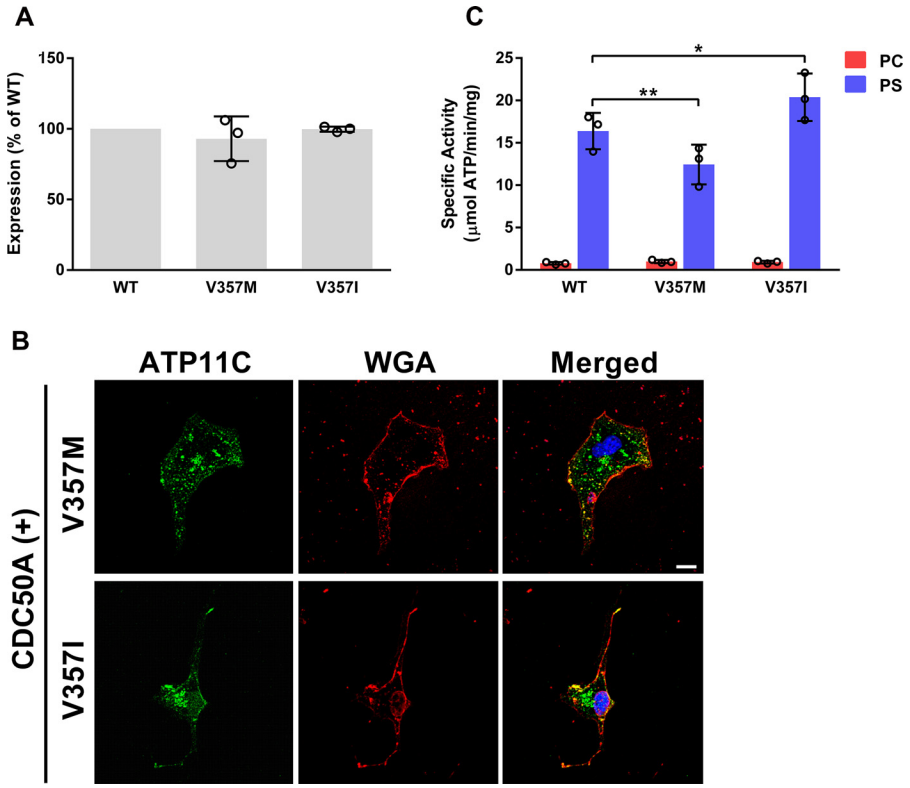

Figure 6. Expression, localization, and specific activity of ATP11C V357M mutant corresponding to I376M in ATP8A2. *A*, immunoaffinity-purified WT ATP11C–CDC50A complexes were quantified from Western blots. Expression of the mutants relative to WT expression is shown. ATP11C mutants all were expressed at levels comparable with WT ATP11C. Data are the average values with *error bars* representing ± S.D. *B*, immunofluorescence micrographs of V357M and V357I mutants coexpressed with CDC50A and labeled for ATP11C mutants (*green*) and WGA (*red*). *Scale bar*, 10 μm. *C*, ATPase activities of ATP11C mutants were measured in 100% DOPC (*PC*) and 80% DOPC and 20% DOPS (*PS*). Although a significant increase in ATPase activity was evident in DOPS, relatively small differences were observed in the PS-activated ATPase activity of the mutants. Data are the average values with *error bars* representing ± S.D. for $n = 3$. *, $p = 0.0266$ for WT *versus* V357I; **, $p = 0.0014$ for WT *versus* V357M.

teins, and ATP8B subfamily members that can use CDC50B as well as CDC50A, were not present in this proteomic study, consistent with the view that ATP11A–C are the only P4-ATPases present in human RBCs.

The finding that ATP11C is the most abundant P4-ATPase in human RBCs is consistent with early studies showing that labeled PS and PE are selectively transported across RBC plasma membrane to generate aminophospholipid asymmetry (23, 26, 28). The functional properties of ATP11A–C recently have been investigated. Their ATPase activities are activated by PS and to a lesser extent PE but not PC (38, 53, 54). Activation of their ATPase activity by PS and PE correlates with the ATP-dependent flipping of PS and PE across membranes as documented using fluorescently labeled phospholipids in cell-based assays (53) and reconstituted proteoliposome systems (38).

Genetic studies have indicated that ATP11C plays a key role in the development and maintenance of blood and liver in mice. A number of strains with mutations in the *Atp11c* gene on the X chromosome were identified in mice subjected to *N*-ethyl-*N*-nitrosourea–induced mutagenesis (15, 44). These mice were normal in their appearance and behavior but displayed defects in B-cell differentiation, anemia, hyperbilirubinemia, cholestasis, and hepatocellular carcinoma. RBCs of ATP11C-deficient mice have also been reported to have abnormal shapes, a reduced life span, and increased exposure of PS on their surface (12). Several strains of *Atp11c* mutant mice had premature termination mutations, resulting in the absence of a functional ATP11C protein. The "spelling" mouse with similar phenotypic traits has an I355K missense mutation (15). Using heterologous expression, we have shown that the I355K mutation does not affect the global structure of ATP11C because the expression level and trafficking of this mutant to the plasma membrane of cells were similar to those of WT ATP11C. Instead, the I355K mutation abolished the functional activity of ATP11C as determined in PS-stimulated ATPase activity assays. Because substitution of isoleucine at position 355 with valine, but not alanine, retains the PS-stimulated ATPase activity of ATP11C, a bulky hydrophobic residue appears to be required at residue 355 for optimal activity. This is further supported by phylogenetic analysis, which indicates that either isoleucine or valine occupies this position in all other P4-ATPases, including yeast Drs2 and Dnf1 (Fig. 7). Interestingly, other P-type ATPases, including sarcoplasmic Ca-ATPase, Na/K-ATPase, and H-ATPase, also have hydrophobic residues at the corresponding position, suggesting that a hydrophobic residue is important in establishing contacts important for the structure–function relationship of these P-type ATPases.

Isoleucine at position 355 in mouse ATP11C occurs within a highly conserved (I/V)P(I/V) motif within predicted TM4 of P4-ATPases (1). An I376M mutation in the downstream hydrophobic residue of this motif in ATP8A2 has been linked to a severe developmental neurological disorder known as CAMRQ

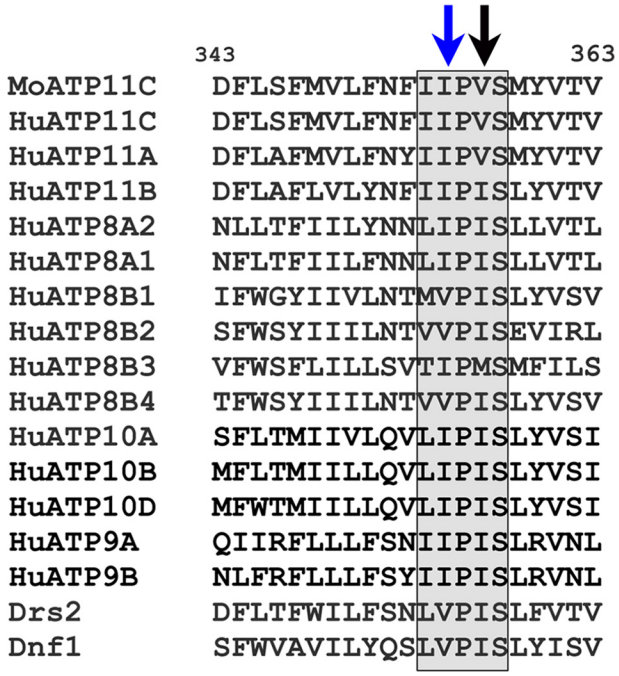

Figure 7. Sequence alignment of predicted TM4 of the mouse ATP11C and 14 human P4-ATPase family members along with yeast P4-ATPases Drs2 and Dnf1. The *boxed* area shows the conserved motif within TM4 that harbors mutations in the hydrophobic residues Ile or Val that flank proline ((I/V)P(I/V)). In mouse (*Mo*) ATP11C, an isoleucine to lysine mutation (I355K; *blue arrow*) results in loss in function of ATP11C and is associated with liver and blood disorders. In human (*Hu*) ATP8A2, an isoleucine to methionine mutation (I376M; *black arrow*) causes CAMRQ.

(17). Functional studies indicate that ATP8A2 I376M mutant (I364M in bovine ATP8A2) is largely devoid of PS-activated ATPase and ATP-dependent PS flippase activities (45, 49). We sought to determine whether a similar mutation (V357M) abolished the activity of ATP11C. Interestingly, our studies show that substitution of valine at 357 for methionine in this motif reduced the PS-activated ATPase activity of ATP11C by only 24%. Although ATP11C and ATP8A2 display similar domain organization and phospholipid transport specificity, apparently these transporters display subtle differences in amino acid contacts within the hydrophobic cavity formed in part by this motif, allowing functional activity of valine to methionine mutation in ATP11C but not isoleucine to methionine in ATP8A2. Indeed, ATP8B3, another P4-ATPase that has been suggested to transport PS, has a methionine at this position (Fig. 7).

A mild form of congenital hemolytic anemia in a male patient was recently linked to a T418N mutation in ATP11C. The RBCs of this patient appeared normal but exhibited a 10-fold decrease in PS internalization. PS was localized on the inner leaflet of the majority of mature cells similar to control cells, but senescent cells displayed PS on their surface. Our studies on the corresponding T415N mutation of mouse ATP11C indicate that this mutation causes significant protein misfolding based on the low expression and an increased retention in the ER of transfected cells as viewed by immunofluorescence microscopy. The fraction that was solubilized by CHAPS and purified by immunoaffinity chromatography assembled with CDC50A and displayed 33% of the PS-activated ATPase activity observed for WT ATP11C. Substitution of the threonine at 415 for alanine also caused lower expression, partial mislocalization in cells, and markedly reduced PS-activated ATPase activity of ATP11C, whereas substitution with serine had no significant effect. These results suggest that the polar hydroxyl side chain at position 415 is an important determinant for protein folding and activity of ATP11C. A detailed analysis of conserved and nonconserved mutations within the DKTGTLT motif in the sarcoplasmic reticulum Ca^{2+}-ATPase (SERCA) has also documented the importance of a polar hydroxyl group at position 357, corresponding to position 415 of mouse ATP11C (55, 56). In this work, deficiency of ATP binding and phosphorylation were demonstrated for T357A. It is likely that a similar inability of the T415A mutant to be efficiently phosphorylated by ATP is part of the underlying reason for the low activity and expression. The phosphoenzyme (E2P) is known to exhibit higher affinity for the CDC50 subunit than the dephosphoenzyme (36). It is possible that the T415A mutation alters the interaction of ATP11C with CDC50A, resulting in lower activity and expression.

It is of interest to note that the loss-of-function mutations in ATP11C result in different phenotypic characteristics in mice and humans. In mice, null mutations and the complete loss-of-function I355K missense mutation as shown here cause B-cell differentiation, hyperbilirubinemia, cholestasis, and hepatocellular carcinoma along with altered red blood cell shape and reduced RBC survival associated with anemia (12, 16, 44). This is consistent with the high content of ATP11C in murine liver (38) and its relative abundance in red blood cells as shown in this study. Interestingly, the relatively high content of ATP8A1 in murine RBCs does not appear to compensate for the loss of function in ATP11C. It is possible that ATP8A1 is present in a largely inactive state in mouse RBCs. In contrast, the human patient with the T418N mutation in ATP11C displays a mild form of congenital hemolytic anemia. The residual activity of this mutant and/or the presence of low-abundance ATP11A and ATP11B in human RBCs as determined here may mitigate the more severe phenotypes observed in mutant mice. Alternatively, ATP11C may play a more important role in murine than human physiology. Further studies are needed to resolve the apparent difference in disease phenotypes in mice and humans exhibiting a loss in ATP11C activity. In either case, the loss in function of ATP11C together with activation of scramblases enables PS to become exposed on the surface of RBCs, triggering removal of these cells by phagocytosis and anemia.

Experimental procedures

Materials

The following phospholipids were obtained from Avanti Polar Lipids (Alabaster, AL): DOPC, DOPS, 1,2-dioleoyl-*sn*-glycero-3-phosphoethanolamine (DOPE), and porcine brain polar lipids. The 7F4 (Ac-AKDEVDGGP) and 1D4 (Ac-TETSQVAPA) peptides were purchased from Biomatik (Cambridge, Ontario, Canada), restriction enzymes were from New England Biolabs (Ipswich, MA), porcine-modified trypsin was from Promega (Nepean, Ontario, Canada), and endopeptidase Lys-C was from Wako Chemicals (Osaka, Japan). CHAPS and

Mega-10 were purchased from Anatrace (Maumee, OH). The rabbit ATP8A1 antibody was obtained from Proteintech. mAb Cdc50–7F4 to CDC50A was produced in-house as described previously (37). The Rho-1D4 mAb produced in-house (57) was obtained from University of British Columbia through Flintbox (UBC). Secondary goat anti-rabbit or anti-mouse Ig antibodies conjugated to horseradish peroxidase were obtained from Millipore-Sigma. Secondary goat anti-mouse antibody conjugated with IRDye 680 was obtained from LI-COR Biosciences. Purified Cdc50–7F4 and Rho-1D4 monoclonal antibodies were directly coupled to CNBr-activated Sepharose 2B at about 1.5 mg/ml of beads as described previously (37).

Preparation of RBC membranes

Human and mouse blood was collected in EDTA-containing tubes in accordance with the approval of the University of British Columbia Institutional Ethics and Animal Care Committees. In the case of obtaining human RBCs, studies abide by the Declaration of Helsinki principles. RBCs were isolated from serum, and white cells were removed as described previously (50, 51). RBC membranes were prepared from hypotonically lysed RBCs according to the method of Dodge *et al.* (58). Protein concentrations of the RBC membranes (~2–3 mg/ml protein) were determined using the Bio-Rad Protein Assay kit.

Immunoaffinity purification of P4-ATPase–CDC50A complexes from RBC membranes

Typically 1.5 ml of RBC membranes (2–3 mg/ml protein) in 5 mM sodium phosphate buffer (pH 7.4) was added to 6 ml of solubilization buffer consisting of 3% CHAPS, 1% Mega-10, ProteaseArrest, and 5 mg of brain polar lipid in phosphate-buffered saline (PBS). After stirring at 4 °C for 30 min, the solution was centrifuged at 50,000 rpm for 30 min in a Beckman TLA110 rotor. The supernatant was collected from the clear pellet (mainly spectrin cytoskeletal matrix) and added to 75 μl of Cdc50–7F4–Sepharose pre-equilibrated in column buffer (10 mM CHAPS, 0.5% Mega-10, 40 mM Tris (pH 7.4), 150 mM NaCl, 5 mM $MgCl_2$, and 1 mM DTT). The sample was mixed on a rotation platform at 4 °C for 1 h. The immunoaffinity matrix was subsequently washed six times with 500 μl of column buffer. The bound protein was eluted twice in 100 μl of the same buffer containing 0.2 mg/ml 7F4 peptide. The eluted samples were analyzed by SDS–gel electrophoresis followed by Western blotting or LC-MS/MS. Western blots were labeled with 1:12 diluted hybridoma fluid containing mouse Cdc50–7F4 antibody or 1:1000 diluted rabbit anti-ATP8A1 followed by goat anti-mouse or goat anti-rabbit Ig conjugated to horseradish peroxidase as described previously (38). Labeling was detected using enhanced chemiluminescence (ECL).

Protein identification by LC-MS/MS

The fraction eluted from the immunoaffinity matrix was digested with endopeptidase Lys-C followed by trypsin using the filter-aided sample preparation procedure as described previously (59). The trypsin-digested samples were submitted to the Proteomics Core Facility of Michael Smith Laboratories at the University of British Columbia for mass spectrometric analysis. Briefly, the samples were acidified with 1% TFA and desalted using a C_{18} stop and go extraction tip. Digested peptides were analyzed by a quadrupole-TOF mass spectrometer (Impact II, Bruker Daltonics) coupled to an Easy Nano LC 1000 HPLC (Thermo Fisher Scientific) using an analytical column that was 40–50 cm long with 75-μm-inner-diameter fused silica with an integrated spray tip pulled with P-2000 laser puller (Sutter Instruments), packed with 1.9-μm-diameter Reprosil-Pur C_{18}-AQ beads (Dr. Maisch GmbH) and operated at 50 °C with an in-house-built column heater. Buffer A consisted of 0.1% aqueous formic acid, and buffer B consisted of 0.1% formic acid and 80% (v/v) acetonitrile in water. A standard 60-min peptide separation was done, and the column was washed with 100% buffer B before re-equilibration with buffer A. The Impact II was set to acquire in data-dependent auto-MS/MS mode with inactive focus fragmenting the 20 most abundant ions (one at a time at 18-Hz rate) after each full-range scan from m/z 200 to m/z 2000 at 5-Hz rate. The isolation window for MS/MS was 2–3, depending on the parent ion m/z, and the collision energy ranged from 23 to 65 eV, depending on ion mass and charge. Parent ions were then excluded from MS/MS for the next 0.4 min and reconsidered if their intensity increased more than 5 times. Singly charged ions were excluded from fragmentation.

Data were searched using MaxQuant (v1.5.3.30). The search was performed against a database comprising the protein sequences from UniProt mouse or human entries plus common contaminants with variable modifications of methionine oxidation and *N*-acetylation of the proteins. Only those peptides exceeding the individually calculated 99% confidence limit (as opposed to the average limit for the whole experiment) were considered as accurately identified. The MS proteomics data have been deposited to the ProteomeXchange Consortium via the PRIDE (1) partner repository with the dataset identifier PXD011841.

Mouse ATP11C WT and mutant constructs

Mouse cDNA of ATP11C was purchased from Open Biosystems (IMAGE: 30843359) and subcloned into pcDNA3 vector with a C-terminal 1D4 tag as described previously (38). The ATP11C dephosphorylation-deficient mutant E181Q, disease-associated, and related mutants I355K, I355A, I355V, T415N, T415S, T415A, V357M, and V357I were generated by site-directed mutagenesis. A clone of mouse CDC50A was obtained from OriGene (clone MC200840). The accession numbers for mouse ATP11C DNA and protein were NM_001037863.2 and Q9QZW0, respectively.

Cell culture and transfection

HEK293T cells were grown in Dulbecco's modified Eagle's complete medium containing 8% bovine growth serum (Thermo Scientific), 2 mM L-glutamine, 100 units/ml penicillin, 100 μg/ml streptomycin, and 0.25 μg/ml amphotericin B (Gibco) and seeded 24 h prior to transfection. Cells were transfected at 70% confluence with 10 μg of total DNA and 30 μg of polyethylenimine (PEI) MAX 40,000 transfection reagent (Polysciences, Inc., catalog number 24765-1)/100-mm dish of cells. For immunoaffinity purification and ATPase activity assay, WT ATP11C and all mutants were cotransfected with

CDC50A. For immunofluorescence imaging, COS-7 cells were maintained in Dulbecco's modified Eagle's complete medium and seeded on coverslips placed in 6-well tissue culture plates 24 h before transfection. A total DNA of 1 μg of ATP11C with or without CDC50A was transfected with 3 μg of PolyJet transfection reagent (Signagen, catalog number SL100688)/coverslip.

Immunoaffinity purification of ATP11C

Transiently transfected cells were harvested 48 h after transfection by centrifugation at 1000 rpm for 5 min. Cell pellets were resuspended and solubilized in solubilization buffer (50 mM HEPES-NaOH (pH 7.5), 150 mM NaCl, 5 mM $MgCl_2$, 10% glycerol, 1 mM DTT, 20 mM CHAPS, 0.5 mg/ml DOPC, and ProteaseArrest) by stirring for 30 min at 4 °C. The soluble fraction was collected after centrifugation at 40,000 rpm for 12 min at 4 °C using a TLA-110 rotor in a Beckman Optima ultracentrifuge and incubated for 1 h at 4 °C with Rho-1D4–Sepharose 2B beads prewashed three times with wash buffer (50 mM HEPES-NaOH (pH 7.5), 150 mM NaCl, 5 mM $MgCl_2$, 10% glycerol, 1 mM DTT, and 10 mM CHAPS). After binding, the beads were washed six times with column buffer (50 mM HEPES-NaOH (pH 7.5), 150 mM NaCl, 5 mM $MgCl_2$, 10% glycerol, 1 mM DTT, 10 mM CHAPS, and 0.5 mg/ml DOPC). The bound proteins were eluted twice with 50 μl of column buffer containing 0.5 mg/ml 1D4 peptide by gentle rotation for 30 min at 17 °C in a centrifuge spin column followed by low-speed centrifugation. The purified proteins were then loaded onto an SDS-PAGE gel with known amounts of BSA standards, and the gel was stained with Coomassie Blue to determine the concentration of ATP11C in each preparation.

Expression analysis of ATP11C

Purified WT and mutant ATP11C proteins were loaded onto an SDS-PAGE gel and transferred onto Immobilon FL membranes (Millipore). Membranes were blocked with 1% milk in PBS for 30 min and incubated with Rho-1D4 monoclonal hybridoma culture fluid diluted 1:100 or Cdc50–7F4 diluted 1:12 for 2 h at room temperature. After washing with PBS/T (PBS containing 0.05% Tween 20) three times, membranes were incubated with goat anti-mouse Ig secondary antibody conjugated with IRDye 680 diluted at 1:20,000 in PBS/T with 0.5% milk for 1 h at room temperature and washed three more times in PBS/T. Images were then taken with the Odyssey® Imaging System (LI-COR Biosciences), and intensity of the bands corresponding to purified ATP11C proteins was quantified and compared with the WT expression level.

ATPase activity assay

DOPC or DOPS at 25 mg/ml was dried under N_2 and resuspended at 5 mg/ml in assay buffer (50 mM HEPES-NaOH (pH 7.5), 150 mM NaCl, 12.5 mM $MgCl_2$, 1 mM DTT, and 10 mM CHAPS). Each ATPase reaction contained 10 μl of immunoaffinity-purified ATP11C proteins in detergent, 12.5 μl of 5 mg/ml resuspended lipids, and 2.5 μl of 50 mM ATP diluted in assay buffer to make up to 25 μl in volume. For the single-point assay, 5 mg/ml resuspended lipids contained either 100% DOPC or 20% DOPS and 80% DOPC. For the PS titration assay, resuspended DOPC with increasing concentrations of DOPS was mixed as designated for each point. The ATPase reactions were carried out at 37 °C for 30 min and terminated by adding 25 μl of 12% SDS. For negative controls, 25 μl of 12% SDS was added to the reactions before the incubation at 37 °C. The amount of phosphate hydrolyzed was measured by a colorimetric method as described previously (7). Briefly, each ATPase reaction was incubated with 75 μl of solution D (6% ascorbic acid and 1% ammonium molybdate in 1 N HCl) for 10 min followed by 120 μl of solution E (2% sodium citrate, 2% sodium meta-arsenite, and 2% acetic acid) and transferred into one well on a 96-well plate. Absorbance of the reactions at 850 nm was measured with a microtiter plate reader and compared with the readings of known phosphate concentrations plotted on a standard curve to calculate the specific activity (μmol of P_i released/min/mg of protein). Measurements were done in triplicate. Kinetic parameters, including curve fitting and statistical analysis, were determined using Prism 7 software. Data were analyzed from two or more separate independent experiments.

Immunofluorescence analysis of ATP11C

At 48 h post-transfection, live cells on coverslips were washed twice with ice-cold Hanks' balanced salt solution and incubated at 4 °C for 15 min with WGA conjugated to Alexa Fluor® 594 (Invitrogen) diluted to 5.0 μg/ml in Hanks' balanced salt solution. After washing with PB buffer (100 mM phosphate buffer (pH 7.4)) three times, cells were fixed with 4% paraformaldehyde and permeabilized with 10% normal goat serum and 0.2% Triton X-100. The cells were then labeled with Rho-1D4 monoclonal hybridoma culture fluid diluted 1:100. In some experiments where WGA was not used, fixed and permeabilized cells were labeled with Rho-1D4 mAb and a polyclonal antibody against calnexin (Abcam, ab13504) at 1:200 dilution for 2 h at room temperature. Cells were washed with PB buffer three times before labeling with 4′,6-diamidino-2-phenylindole (DAPI) (diluted 1:1000), Alexa Fluor 488–conjugated goat anti-mouse, and, for calnexin staining, Alexa Fluor 594–conjugated goat anti-rabbit secondary antibodies for 1 h. The coverslips were mounted on glass slides with Mowiol mounting solution and examined on a Zeiss LSM 700 confocal scanning microscope.

Cell surface biotinylation assay

Transfected HEK293T cells were first washed three times with ice-cold PBS containing 0.5 mM $CaCl_2$ and 1 mM $MgCl_2$ (PBS++) and then incubated with 0.5 mg/ml sulfo-NHS-LC-biotin (Thermo Scientific) in PBS++ at 4 °C for 30 min. The biotinylation labeling was quenched by washing cells with ice-cold PBS++ containing 100 mM glycine and 25 mM Tris two times followed by washing with PBS++ two more times. The cells were solubilized in solubilization buffer (50 mM HEPES-NaOH (pH 7.4), 150 mM NaCl, 5 mM $MgCl_2$, 10% glycerol, 1 mM DTT, 20 mM CHAPS, 0.5 mg/ml DOPC, and ProteaseArrest) for 30 min at 4 °C and centrifuged at 40,000 rpm at 4 °C for 12 min in an Optima ultracentrifuge. The supernatant was incubated with 50 μl of streptavidin-agarose beads (Thermo Scientific) pre-equilibrated with column buffer (50 mM HEPES-NaOH (pH 7.4), 150 mM NaCl, 5 mM $MgCl_2$, 10% glycerol, 1 mM

DTT, 10 mM CHAPS, and 0.5 mg/ml DOPC) at 4 °C for 1 h. After washing the beads six times with column buffer, bound proteins were eluted from each column with 30 μl of 2× SDS-PAGE sample buffer supplemented with β-mercaptoethanol. Samples before and after binding to the streptavidin beads were subjected to SDS-PAGE for Western blot analysis. Blots were labeled for ATP8A2 with the Rho-1D4 antibody (1:100), and Na^+/K^+-ATPase α subunit ascites fluid (1:2000) (Developmental Studies Hybridoma Bank).

Data analysis

Kinetic parameters, including curve fitting and statistical analysis, were determined using Prism 7 software. Data were analyzed from two or more separate independent experiments. Student's paired *t* test was used to obtain *p* values for expression studies.

Author contributions—A. Y. L., L. L. M., J. W., and R. S. M. data curation; A. Y. L., L. L. M., J. W., and R. S. M. formal analysis; A. Y. L., L. L. M., and R. S. M. validation; A. Y. L., L. L. M., and J. W. investigation; A. Y. L., L. L. M., and R. S. M. visualization; A. Y. L., L. L. M., and J. W. methodology; A. Y. L. and R. S. M. writing-original draft; A. Y. L., L. L. M., J. W., J. P. A., and R. S. M. writing-review and editing; R. S. M. conceptualization; R. S. M. supervision; R. S. M. funding acquisition; R. S. M. project administration.

Acknowledgments—We thank Karen Chang for technical assistance in producing some of the mutants and Jenny Moon and Dr. Leonard Foster of the Proteomic Core Facility for assistance with the MS.

References

1. Andersen, J. P., Vestergaard, A. L., Mikkelsen, S. A., Mogensen, L. S., Chalat, M., and Molday, R. S. (2016) P4-ATPases as phospholipid flippases—structure, function, and enigmas. *Front Physiol.* **7,** 275 CrossRef Medline
2. Sebastian, T. T., Baldridge, R. D., Xu, P., and Graham, T. R. (2012) Phospholipid flippases: building asymmetric membranes and transport vesicles. *Biochim. Biophys. Acta* **1821,** 1068–1077 CrossRef Medline
3. Lopez-Marques, R. L., Theorin, L., Palmgren, M. G., and Pomorski, T. G. (2014) P4-ATPases: lipid flippases in cell membranes. *Pflugers Arch.* **466,** 1227–1240 CrossRef Medline
4. Kobayashi, T., and Menon, A. K. (2018) Transbilayer lipid asymmetry. *Curr. Biol.* **28,** R386–R391 CrossRef Medline
5. Coleman, J. A., Quazi, F., and Molday, R. S. (2013) Mammalian P4-ATPases and ABC transporters and their role in phospholipid transport. *Biochim. Biophys. Acta* **1831,** 555–574 CrossRef Medline
6. López-Marqués, R. L., Poulsen, L. R., Bailly, A., Geisler, M., Pomorski, T. G., and Palmgren, M. G. (2015) Structure and mechanism of ATP-dependent phospholipid transporters. *Biochim. Biophys. Acta* **1850,** 461–475 CrossRef Medline
7. Coleman, J. A., Kwok, M. C., and Molday, R. S. (2009) Localization, purification, and functional reconstitution of the P4-ATPase Atp8a2, a phosphatidylserine flippase in photoreceptor disc membranes. *J. Biol. Chem.* **284,** 32670–32679 CrossRef Medline
8. Quazi, F., and Molday, R. S. (2013) Differential phospholipid substrates and directional transport by ATP-binding cassette proteins ABCA1, ABCA7, and ABCA4 and disease-causing mutants. *J. Biol. Chem.* **288,** 34414–34426 CrossRef Medline
9. Williamson, P. (2015) Phospholipid scramblases. *Lipid Insights* **8,** 41–44 CrossRef Medline
10. Bevers, E. M., and Williamson, P. L. (2016) Getting to the outer leaflet: physiology of phosphatidylserine exposure at the plasma membrane. *Physiol. Rev.* **96,** 605–645 CrossRef Medline
11. Zhu, X., Libby, R. T., de Vries, W. N., Smith, R. S., Wright, D. L., Bronson, R. T., Seburn, K. L., and John, S. W. (2012) Mutations in a P-type ATPase gene cause axonal degeneration. *PLoS Genet.* **8,** e1002853 CrossRef Medline
12. Yabas, M., Coupland, L. A., Cromer, D., Winterberg, M., Teoh, N. C., D'Rozario, J., Kirk, K., Bröer, S., Parish, C. R., and Enders, A. (2014) Mice deficient in the putative phospholipid flippase ATP11C exhibit altered erythrocyte shape, anemia, and reduced erythrocyte life span. *J. Biol. Chem.* **289,** 19531–19537 CrossRef Medline
13. van der Mark, V. A., Elferink, R. P., and Paulusma, C. C. (2013) P4 ATPases: flippases in health and disease. *Int. J. Mol. Sci.* **14,** 7897–7922 CrossRef Medline
14. Stapelbroek, J. M., Peters, T. A., van Beurden, D. H., Curfs, J. H., Joosten, A., Beynon, A. J., van Leeuwen, B. M., van der Velden, L. M., Bull, L., Oude Elferink, R. P., van Zanten, B. A., Klomp, L. W., and Houwen, R. H. (2009) ATP8B1 is essential for maintaining normal hearing. *Proc. Natl. Acad. Sci. U.S.A.* **106,** 9709–9714 CrossRef Medline
15. Siggs, O. M., Arnold, C. N., Huber, C., Pirie, E., Xia, Y., Lin, P., Nemazee, D., and Beutler, B. (2011) The P4-type ATPase ATP11C is essential for B lymphopoiesis in adult bone marrow. *Nat. Immunol.* **12,** 434–440 CrossRef Medline
16. Siggs, O. M., Schnabl, B., Webb, B., and Beutler, B. (2011) X-linked cholestasis in mouse due to mutations of the P4-ATPase ATP11C. *Proc. Natl. Acad. Sci. U.S.A.* **108,** 7890–7895 CrossRef Medline
17. Onat, O. E., Gulsuner, S., Bilguvar, K., Nazli Basak, A., Topaloglu, H., Tan, M., Tan, U., Gunel, M., and Ozcelik, T. (2013) Missense mutation in the ATPase, aminophospholipid transporter protein ATP8A2 is associated with cerebellar atrophy and quadrupedal locomotion. *Eur. J. Hum. Genet.* **21,** 281–285 CrossRef Medline
18. Coleman, J. A., Zhu, X., Djajadi, H. R., Molday, L. L., Smith, R. S., Libby, R. T., John, S. W., and Molday, R. S. (2014) Phospholipid flippase ATP8A2 is required for normal visual and auditory function and photoreceptor and spiral ganglion cell survival. *J. Cell Sci.* **127,** 1138–1149 CrossRef Medline
19. Castoldi, E., Collins, P. W., Williamson, P. L., and Bevers, E. M. (2011) Compound heterozygosity for 2 novel TMEM16F mutations in a patient with Scott syndrome. *Blood* **117,** 4399–4400 CrossRef Medline
20. McMillan, H. J., Telegrafi, A., Singleton, A., Cho, M. T., Lelli, D., Lynn, F. C., Griffin, J., Asamoah, A., Rinne, T., Erasmus, C. E., Koolen, D. A., Haaxma, C. A., Keren, B., Doummar, D., Mignot, C., *et al.* (2018) Recessive mutations in ATP8A2 cause severe hypotonia, cognitive impairment, hyperkinetic movement disorders and progressive optic atrophy. *Orphanet J. Rare Dis.* **13,** 86 CrossRef Medline
21. Bretscher, M. S. (1972) Asymmetrical lipid bilayer structure for biological membranes. *Nat. New Biol.* **236,** 11–12 Medline
22. Daleke, D. L. (2003) Regulation of transbilayer plasma membrane phospholipid asymmetry. *J. Lipid Res.* **44,** 233–242 CrossRef Medline
23. Seigneuret, M., and Devaux, P. F. (1984) ATP-dependent asymmetric distribution of spin-labeled phospholipids in the erythrocyte membrane: relation to shape changes. *Proc. Natl. Acad. Sci. U.S.A.* **81,** 3751–3755 CrossRef Medline
24. Zachowski, A. (1993) Phospholipids in animal eukaryotic membranes: transverse asymmetry and movement. *Biochem. J.* **294,** 1–14 CrossRef Medline
25. Zachowski, A., Favre, E., Cribier, S., Hervé, P., and Devaux, P. F. (1986) Outside-inside translocation of aminophospholipids in the human erythrocyte membrane is mediated by a specific enzyme. *Biochemistry* **25,** 2585–2590 CrossRef Medline
26. Daleke, D. L., and Huestis, W. H. (1985) Incorporation and translocation of aminophospholipids in human erythrocytes. *Biochemistry* **24,** 5406–5416 CrossRef Medline
27. Morrot, G., Hervé, P., Zachowski, A., Fellmann, P., and Devaux, P. F. (1989) Aminophospholipid translocase of human erythrocytes: phospholipid substrate specificity and effect of cholesterol. *Biochemistry* **28,** 3456–3462 CrossRef Medline
28. Auland, M. E., Roufogalis, B. D., Devaux, P. F., and Zachowski, A. (1994) Reconstitution of ATP-dependent aminophospholipid translocation in proteoliposomes. *Proc. Natl. Acad. Sci. U.S.A.* **91,** 10938–10942 CrossRef Medline

29. Zachowski, A., Henry, J. P., and Devaux, P. F. (1989) Control of transmembrane lipid asymmetry in chromaffin granules by an ATP-dependent protein. *Nature* **340,** 75–76 CrossRef Medline
30. Tang, X., Halleck, M. S., Schlegel, R. A., and Williamson, P. (1996) A subfamily of P-type ATPases with aminophospholipid transporting activity. *Science* **272,** 1495–1497 CrossRef Medline
31. Mouro, I., Halleck, M. S., Schlegel, R. A., Mattei, M. G., Williamson, P., Zachowski, A., Devaux, P., Cartron, J. P., and Colin, Y. (1999) Cloning, expression, and chromosomal mapping of a human ATPase II gene, member of the third subfamily of P-type ATPases and orthologous to the presumed bovine and murine aminophospholipid translocase. *Biochem. Biophys. Res. Commun.* **257,** 333–339 CrossRef Medline
32. Soupene, E., Kemaladewi, D. U., and Kuypers, F. A. (2008) ATP8A1 activity and phosphatidylserine transbilayer movement. *J. Receptor Ligand Channel Res.* **1,** 1–10 CrossRef Medline
33. Levano, K., Punia, V., Raghunath, M., Debata, P. R., Curcio, G. M., Mogha, A., Purkayastha, S., McCloskey, D., Fata, J., and Banerjee, P. (2012) Atp8a1 deficiency is associated with phosphatidylserine externalization in hippocampus and delayed hippocampus-dependent learning. *J. Neurochem.* **120,** 302–313 CrossRef Medline
34. Arashiki, N., Takakuwa, Y., Mohandas, N., Hale, J., Yoshida, K., Ogura, H., Utsugisawa, T., Ohga, S., Miyano, S., Ogawa, S., Kojima, S., and Kanno, H. (2016) ATP11C is a major flippase in human erythrocytes and its defect causes congenital hemolytic anemia. *Haematologica* **101,** 559–565 CrossRef Medline
35. Saito, K., Fujimura-Kamada, K., Furuta, N., Kato, U., Umeda, M., and Tanaka, K. (2004) Cdc50p, a protein required for polarized growth, associates with the Drs2p P-type ATPase implicated in phospholipid translocation in Saccharomyces cerevisiae. *Mol. Biol. Cell* **15,** 3418–3432 CrossRef Medline
36. Lenoir, G., Williamson, P., Puts, C. F., and Holthuis, J. C. (2009) Cdc50p plays a vital role in the ATPase reaction cycle of the putative aminophospholipid transporter Drs2p. *J. Biol. Chem.* **284,** 17956–17967 CrossRef Medline
37. Coleman, J. A., and Molday, R. S. (2011) Critical role of the β-subunit CDC50A in the stable expression, assembly, subcellular localization, and lipid transport activity of the P4-ATPase ATP8A2. *J. Biol. Chem.* **286,** 17205–17216 CrossRef Medline
38. Wang, J., Molday, L. L., Hii, T., Coleman, J. A., Wen, T., Andersen, J. P., and Molday, R. S. (2018) Proteomic analysis and functional characterization of P4-ATPase phospholipid flippases from murine tissues. *Sci. Rep.* **8,** 10795 CrossRef Medline
39. Katoh, Y., and Katoh, M. (2004) Identification and characterization of CDC50A, CDC50B and CDC50C genes *in silico*. *Oncol. Rep.* **12,** 939–943 Medline
40. Paulusma, C. C., Folmer, D. E., Ho-Mok, K. S., de Waart, D. R., Hilarius, P. M., Verhoeven, A. J., and Oude Elferink, R. P. (2008) ATP8B1 requires an accessory protein for endoplasmic reticulum exit and plasma membrane lipid flippase activity. *Hepatology* **47,** 268–278 CrossRef Medline
41. Bryde, S., Hennrich, H., Verhulst, P. M., Devaux, P. F., Lenoir, G., and Holthuis, J. C. (2010) CDC50 proteins are critical components of the human class-1 P4-ATPase transport machinery. *J. Biol. Chem.* **285,** 40562–40572 CrossRef Medline
42. van der Velden, L. M., Wichers, C. G., van Breevoort, A. E., Coleman, J. A., Molday, R. S., Berger, R., Klomp, L. W., and van de Graaf, S. F. (2010) Heteromeric interactions required for abundance and subcellular localization of human CDC50 proteins and class 1 P4-ATPases. *J. Biol. Chem.* **285,** 40088–40096 CrossRef Medline
43. Takatsu, H., Baba, K., Shima, T., Umino, H., Kato, U., Umeda, M., Nakayama, K., and Shin, H. W. (2011) ATP9B, a P4-ATPase (a putative aminophospholipid translocase), localizes to the trans-Golgi network in a CDC50 protein-independent manner. *J. Biol. Chem.* **286,** 38159–38167 CrossRef Medline
44. Yabas, M., Teh, C. E., Frankenreiter, S., Lal, D., Roots, C. M., Whittle, B., Andrews, D. T., Zhang, Y., Teoh, N. C., Sprent, J., Tze, L. E., Kucharska, E. M., Kofler, J., Farell, G. C., Bröer, S., *et al.* (2011) ATP11C is critical for the internalization of phosphatidylserine and differentiation of B lymphocytes. *Nat. Immunol.* **12,** 441–449 CrossRef Medline
45. Vestergaard, A. L., Coleman, J. A., Lemmin, T., Mikkelsen, S. A., Molday, L. L., Vilsen, B., Molday, R. S., Dal Peraro, M., and Andersen, J. P. (2014) Critical roles of isoleucine-364 and adjacent residues in a hydrophobic gate control of phospholipid transport by the mammalian P4-ATPase ATP8A2. *Proc. Natl. Acad. Sci. U.S.A.* **111,** E1334–E1343 CrossRef Medline
46. Vilsen, B., and Andersen, J. P. (1998) Mutation to the glutamate in the fourth membrane segment of Na^+,K^+-ATPase and Ca^{2+}-ATPase affects cation binding from both sides of the membrane and destabilizes the occluded enzyme forms. *Biochemistry* **37,** 10961–10971 CrossRef Medline
47. Olesen, C., Picard, M., Winther, A. M., Gyrup, C., Morth, J. P., Oxvig, C., Møller, J. V., and Nissen, P. (2007) The structural basis of calcium transport by the calcium pump. *Nature* **450,** 1036–1042 CrossRef Medline
48. Møller, J. V., Olesen, C., Winther, A. M., and Nissen, P. (2010) The sarcoplasmic Ca^{2+}-ATPase: design of a perfect chemi-osmotic pump. *Q Rev. Biophys.* **43,** 501–566 CrossRef Medline
49. Lee, S., Uchida, Y., Wang, J., Matsudaira, T., Nakagawa, T., Kishimoto, T., Mukai, K., Inaba, T., Kobayashi, T., Molday, R. S., Taguchi, T., and Arai, H. (2015) Transport through recycling endosomes requires EHD1 recruitment by a phosphatidylserine translocase. *EMBO J.* **34,** 669–688 CrossRef Medline
50. Pasini, E. M., Kirkegaard, M., Salerno, D., Mortensen, P., Mann, M., and Thomas, A. W. (2008) Deep coverage mouse red blood cell proteome: a first comparison with the human red blood cell. *Mol. Cell. Proteomics* **7,** 1317–1330 CrossRef Medline
51. Pasini, E. M., Kirkegaard, M., Mortensen, P., Lutz, H. U., Thomas, A. W., and Mann, M. (2006) In-depth analysis of the membrane and cytosolic proteome of red blood cells. *Blood* **108,** 791–801 CrossRef Medline
52. Bryk, A. H., and Wiąsniewski, J. R. (2017) Quantitative analysis of human red blood cell proteome. *J. Proteome Res.* **16,** 2752–2761 CrossRef Medline
53. Segawa, K., Kurata, S., and Nagata, S. (2016) Human type IV P-type ATPases that work as plasma membrane phospholipid flippases and their regulation by caspase and calcium. *J. Biol. Chem.* **291,** 762–772 CrossRef Medline
54. Ding, J., Wu, Z., Crider, B. P., Ma, Y., Li, X., Slaughter, C., Gong, L., and Xie, X. S. (2000) Identification and functional expression of four isoforms of ATPase II, the putative aminophospholipid translocase. Effect of isoform variation on the ATPase activity and phospholipid specificity. *J. Biol. Chem.* **275,** 23378–23386 CrossRef Medline
55. Maruyama, K., Clarke, D. M., Fujii, J., Inesi, G., Loo, T. W., and MacLennan, D. H. (1989) Functional consequences of alterations to amino acids located in the catalytic center (isoleucine 348 to threonine 357) and nucleotide-binding domain of the Ca^{2+}-ATPase of sarcoplasmic reticulum. *J. Biol. Chem.* **264,** 13038–13042 Medline
56. McIntosh, D. B., Woolley, D. G., MacLennan, D. H., Vilsen, B., and Andersen, J. P. (1999) Interaction of nucleotides with Asp^{351} and the conserved phosphorylation loop of sarcoplasmic reticulum Ca^{2+}-ATPase. *J. Biol. Chem.* **274,** 25227–25236 CrossRef Medline
57. Hodges, R. S., Heaton, R. J., Parker, J. M., Molday, L., and Molday, R. S. (1988) Antigen-antibody interaction. Synthetic peptides define linear antigenic determinants recognized by monoclonal antibodies directed to the cytoplasmic carboxyl terminus of rhodopsin. *J. Biol. Chem.* **263,** 11768–11775 Medline
58. Dodge, J. T., Mitchell, C., and Hanahan, D. J. (1963) The preparation and chemical characteristics of hemoglobin-free ghosts of human erythrocytes. *Arch. Biochem. Biophys.* **100,** 119–130 CrossRef Medline
59. Wiśniewski, J. R., Zougman, A., Nagaraj, N., and Mann, M. (2009) Universal sample preparation method for proteome analysis. *Nat. Methods* **6,** 359–362 CrossRef Medline